NITRATE REDUCTION USING SYNTHESIZED G--NZVI AND G--NZVI--CU PREPAREDFROM OPTIMIZED EXTRACTED POLYPHENOLS FROM SUGANDA LEAVES

Vanessa Denise C. Aguilar, Jerome D.R. Fundano, Jeswino C. Legaspi, Darwin C. Mojica, Janselle Q. Tullao, Alister Mae A. Zafra & Engr. Erison C. Roque[1]

Department of Chemical Engineering, College of Engineering, Adamson University, Ermita, Manila, Philippines

[1]erison.roque@adamson.edu.ph

Abstract

Polyphenols present in Suganda (Plectranthus amboinicus (Lour.) Spreng) extract can reduce the cationic iron to zero valent iron while simultaneously forming nanoparticles. The study involved the phenolic extraction at different solvent concentrations and temperatures. The synthesized Green--Nanoscale Zero Valent Iron (G--nZVI) and Green--Nanoscale Zero Valent Iron -- Copper Bimetal (G--nZVI--Cu) were used to reduce nitrate in water. Scanning Electron Microscopy -- Energy Dispersive X--ray (SEM--EDX) and X--ray Diffraction (XRD) are used to characterize the particles. It was found out that at 35°C and 90% ethanol, the highest phenolic content was obtained. The Analysis of Variance (ANOVA) results showed that the effect of temperature and solvent concentration is significant on the phenolic extraction with a probability value of < 0.0001. The SEM analysis showed that the particles have sizes ranging from 100--150 nm. The EDX analysis showed higher amounts of oxygen ranging from 50--60%, iron having 40--50% weight and copper with nearly 4--5% weight. The green synthesized particles are amorphous in structure, with no clear peak at $2\theta = 45°$. The synthesized particles were successfully used to reduce nitrate in water. Analysis showed that significant amount of nitrate was reduced after 60 minutes, having a removal efficiency of 84.36% and 85.81% for G--nZVI and G--nZVI--Cu, respectively. It was found out that ammonium and nitrogen gas were the main products of the reaction. The results show that G--nZVI and G--nZVI--Cu can be used for the remediation of nitrate in water due to its high removal efficiency.

Keywords: Green Nanoscale Zero Valent Iron (G--nZVI), Green Nanoscale Zero Valent Iron--Copper (G--nZVI--Cu), Total Phenolic Content, Copper (II), Iron (III), Nitrate Reduction

1.0 INTRODUCTION

Nitrate can be retrieved from plant sources as well as from contaminated drinking water. A high concentration of nitrate is dangerous to human health. Methemoglobinemia is one of the dangerous effects of nitrate, where it is converted into nitrite. This can further lead to the formation of methemoglobin, which tightly binds oxygen that leads to deprivation of oxygen in the cells (Follett & Hatfield, 2010). High nitrate concentrations also lead to heart and respiratory problems, even death in severe cases.

Nanoscale zero valent iron is considered as a new technique for water and soil treatment (Crane & Scott, 2012). The morphology of nZVI particle is core--shell structure which contributes to its high reactivity. Synthesis of nanoparticles using green method has fascinated significant consideration in the previous years. Green substances utilization showed numerous advantages including adequate operating conditions (e.g. pressure and temperature) and low energy use (Mohammadlou, Maghsoudi, & Jafarizadeh--Malmiri, 2016).

As green technology emerges in the past few years, nitrate reduction using bimetals has drawn attention because of easier operations, selectivity concerning nontoxic products and higher removal efficiency compared to other physicochemical technologies (Hamid, Bae, Lee, Amin, & Alazba, 2015). Copper metal is recognized to be effective in catalytic reduction of nitrate among other metals (Jung, Bae, & Lee, 2014).

This paper emphasizes on the green synthesis of nano zero valent iron using Fe--Cu bimetal precursor solutions. It is presented as an alternative solution in nitrate removal among different water treatment technologies.

2.0 LITERATURE REVIEW

Nanoscale zero valent iron (nZVI) is an iron in nano size that has a zero valence electron. In ambient conditions, the reactivity of nZVI is high and it is a good catalyst in redox reaction. NZVI is becoming as an apparent option for environmental remediation and hazardous waste treatment aiming primarily chlorinated organic contaminants (Mueller et al., 2012).

NZVI has been known for its effectiveness at stabilization and transformation a wide variety common environmental contaminants by its highly reducing character(Wang, Le, Alvarez, Li, & Liu, 2015). As an outstanding reductant, nZVI has strong points for effective subsurface remediation capacity as follows:

1) Small particle size and large surface per unit mass results to an increase of reactivity
2) Improved efficiency of chlorine removal with nZVI promotes non--toxic for it prevents the incomplete dechlorination
3) Sufficient mobility across porous structures of extensive subsurface environment

4) Ability to coat a layer of second metal onto the surface of Fe^0 for the formation of bimetallic particles like Ni/Fe , Pd/Fe, Cu/Fe and Pt/Fe bimetallic nanoparticles

Green synthesis method is a plant--mediated biological way of synthesizing nanoparticles. One of the most effective methods in this synthesis is by using extracts in different parts of the tree, especially leaf, as it reduces metal ions in a shorter time. Such synthesized nanoparticles are called green NZVI (Pattanayak& Nayak, 2012). The following are the prominent advantages of the green synthesis method:

1) Clean and environmentally friendly
2) Active biological component like enzyme itself acts as a reducing and capping agent, hence, making it more cost--effective
3) The production of large quantities of nanoparticles is scaled up by using small nanoparticles.
4) Significant energy saving for high pressure and high temperature are not required

Oxygen has two functions in NZVI. First, it is the major factor in oxidation of NZVI which is also the reason in reduction of nitrate. The other function of oxygen is the formation of ferric oxides, like Fe_2O_3 and Fe_3O4, which reduces the reactivity of NZVI (Guo et al., 2015). Other compounds in water may also bond with NZVI which also reduces its reactivity. Another setback in using NZVI is its weak subsurface mobility(Carroll, Sleep, Krol, Boparai, & Kocur, 2012).

To solve this problem, an addition of another noble metal, like Ag, Cu, Ni, Pd and Pt, on the surface of NZVI was made which is called to be a bimetallic nanometal (Carroll et al., 2012;; Sparis, Mystrioti, Xenidis, & Papassiopi, 2015). This process can stabilize iron and improves the reduction/oxidation performance through catalytic process (Muradova, Gadjieva, Di, & Vilardi, 2016).

Copper is one of the most used surface modifier metal sand recognized being a mild hydrogenation catalyst(Hosseini et al., 2011). It has a higher reactivity to NO_3^---N than platinum and palladium which increases the amount of reduced nitrate when used with NZVI and lessen the agglomeration and aggregation that happens in NZVI when it is inserted in a permeable media.

3.0 METHODOLOGY

Materials and Methods

Suganda leaves were used as the plant species in the study. Ferric chloride hexahydrate ($FeCl_3 \bullet 6H_2O$) was used as iron precursor. Copper (II) chloride ($CuCl_2$) was used as the bimetal coating. Folin--Ciocalteu reagent and anhydrous sodium carbonate aided the phenolic content determination. The determination of absorbance and construction of calibration curves were generated using Gallic acid.

Extraction was done using 9 cases at varying temperature (25°C, 35°C and 45°C) and solvent concentration (50%, 70% and 90%) using water bath shaker having a 1:10 suganda to solvent ratio for 3 hours. Using Folin--Ciocalteu method, phenolic

content determination of the extracts was performed. Gallic acid was used for the standard curve. The extract with the highest phenolic content was used for the synthesis of G--nZVI and G--nZVI--Cu particles.

Synthesis of the particles was carried out using a triple neck flask, magnetic stirrer and burette. The suganda extract was placed in the burette, having the iron precursors in the triple neck flask. Constant agitation was done with the dropwise addition of the extract. A black suspension was formed, and was filtered afterwards. The black precipitate was further subjected to freeze drying prior to nitrate reduction.

Nitrate reduction was done at a known concentration of Potassium nitrate solution. The synthesized particles were added to the solution while monitoring the pH, ORP and ammonium generation every 15 minutes.

Statistical Treatment

The data gathered from this experiment were statistically treated using Multiple Linear regression, Two Sample T--Test and ANOVA of the General Factorial Model. Multiple Linear Regression was used to determine the linear relationship between the dependent variable, % nitrate reduction, and the independent variables, pH and the ORP. Two sample T--Test was used to compare the data gathered using the G--nZVI particles for nitrate reduction and the data which were gathered in using G--nZVI--Cu. ANOVA of the General Factorial Model was used to determine if the parameters used in the phenolic extraction is statistically significant.

4.0 RESULTS AND DISCUSSION

Effect of Temperature and Solvent Concentration on Phenolic Extraction The relationship of the different concentrations of Gallic acid is directly proportional toits absorbance. The graph also shows the equation of the curve, which is y = 1.6162x + 0.1173 and having R^2 = 0.9957. Since it is close to 1.0, it can be accepted as a linear relationship. The standard curve is used to estimate the phenolic content of the 9 cases.

Table C.1 in the appendix (not attached) shows the graph between the 9 cases extracted with different concentrations and its absorbance. The figure shows that Case 6 has the highest absorbance among all the cases. A mean absorbance with a value of 1.634 in concentration of 1 mg/ml gives the highest value among the others.

Table 1: Average Total Phenolic Content of a 1 mg/ml Sample with Varying Temperature and Solvent Concentration

1 mg/ml	**Solvent Concentration**		
Temperature	**50%**	**70%**	**90%**
25°C	2.760	3.814	8.539
35°C	2.968	7.184	9.281
45°C	1.141	3.744	5.903

Table 2: Average Total Phenolic Content of a 0.5 mg/ml Sample with Varying Temperature and Solvent Concentration

0.5 mg/ml	**Solvent Concentration**		
Temperature	50%	70%	90%
25°C	2.748	3.849	8.547
35°C	3.247	7.137	9.121
45°C	1.114	3.948	6.221

Table 3: Average Total Phenolic Content of a 0.2 mg/ml Sample with Varying Temperature and Solvent Concentration

0.2 mg/ml	**Solvent Concentration**		
Temperature	50%	70%	90%
25°C	2.930	3.899	8.756
35°C	3.157	7.570	9.127
45°C	1.424	3.683	6.168

Table 4: Average Total Phenolic Content of a 0.1 mg/ml Sample with Varying Temperature and Solvent Concentration

0.1 mg/ml	**Solvent Concentration**		
Temperature	50%	70%	90%
25°C	2.539	3.941	8.871
35°C	3.199	6.664	9.118
45°C	1.466	5.034	6.437

Table 5: Average Total Phenolic Content of a 0.05 mg/ml Sample with Varying Temperature and Solvent Concentration

0.05 mg/ml	**Solvent Concentration**		
Temperature	50%	70%	90%
25°C	2.768	3.882	8.336
35°C	3.057	7.470	9.120
45°C	1.572	3.552	6.026

The phenolic content for all of the cases are shown above with different concentration of the sample. The tables above show that the ones who have 90% solvent concentration have the highest value for each of the temperatures. This is due to the higher extract that was extracted from Suganda.

As the temperature increases, the amount of extract that can be obtained also increases due to the heat reduces the permeability of cell walls and polyphenol's diffusion coefficient and extraction solvent solubility also increases (Wissam et al., 2012). The total phenolic content increases as temperature decreases but the TPC in 45°C is lower than in 35°C in all solvent concentration. According to Wissam et al. also, degradation of phenolic compounds at 50°C. 45°C is near to degradation temperature of 50°C, so some of the phenolic compounds might degrade.

The tables above were tested statistically using ANOVA. The results showed that the p--value of temperature and solvent concentration are less than 0.0001. Overall, the data implies that the temperature and the concentration of solvent are significant to the extraction of phenolic compounds.

Characterization of G--nZVI and G--nZVI--Cu Particles

Morphology and Particle Size

The G--NZVI and G--NZVI--Cu particles that were produced were analyzed using the Scanning Electron Microscope (SEM). SEM was used to determine the particle sizes. Table 5 shows the particle sizes of G--NZVI and G--NZVI--Cu obtained using 20,000 magnification.

Table 5: Particle Size of G--nZVI and G--nZVI--Cu

SEM (20,000 magnification)			
Precursor	**Sizes of Particles (nm)**		
	1	**2**	**3**
G--NZVI	124	141	132
G--NZVI--Cu	121	134	131

Figure 1 and 2 show SEM images of a typical nZVI cluster. The nanoparticles form chain--like formations and appear agglomerated due to electrostatic and magnetic interactions (Yan et al., 2010).

The G--nZVI and G--nZVI--Cu particles are black colored and spherical in nature. The basis for nanoscale characterization of both G--NZVI and G--NZVIC particles is 10 nm to 100 nm, but up to 200 nm is acceptable. The particles exhibited an aggregate--like spherical morphology under SEM. It is found out that the G--nZVI and G--nZVI Cu particles are prone to aggregation (Wang et al., 2014). This phenomenon causes decrease of G--nZVI and G--nZVI Cu's stability and mobility. But compared to G--nZVI particles, SEM images showed that G--nZVI--Cu particles have lesser agglomeration. This was due to the copper addition to the G--nZVI surface (Vilardi and Palma, 2016).

4.1 Elemental Analysis

The content of the sample is another factor to consider. By using the Energy Dispersive X--ray Machine (EDX) the constituents of the G--NZVI and G--NZVI--Cu were analyzed in weight concentration. Figure 1 shows the elemental analysis of G--NZVI and Figure 2 shows the elemental analysis of G--NZVI--Cu.

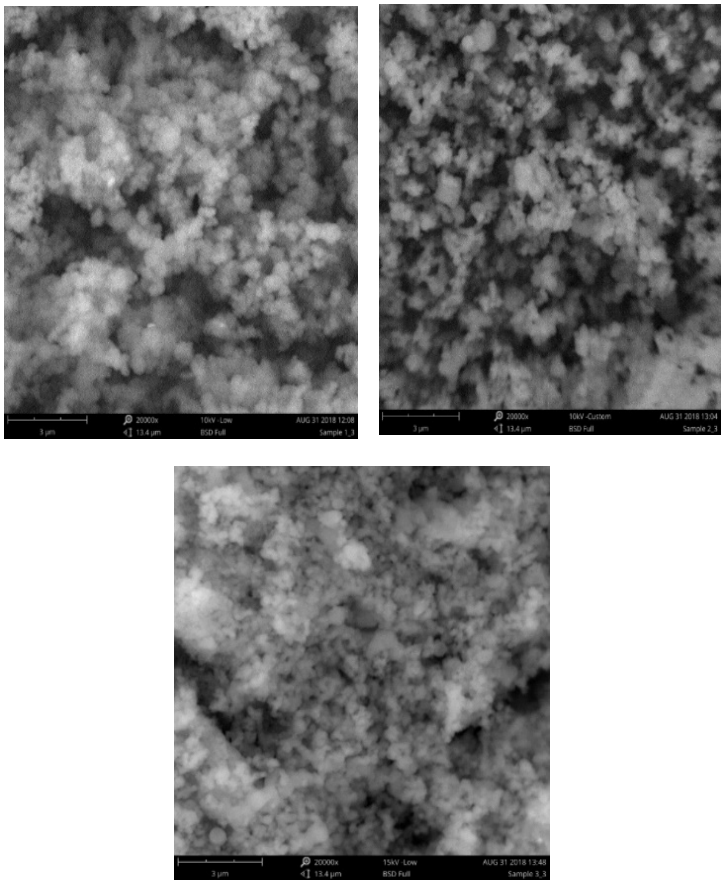

Figure 1: SEM Images of G--nZVI

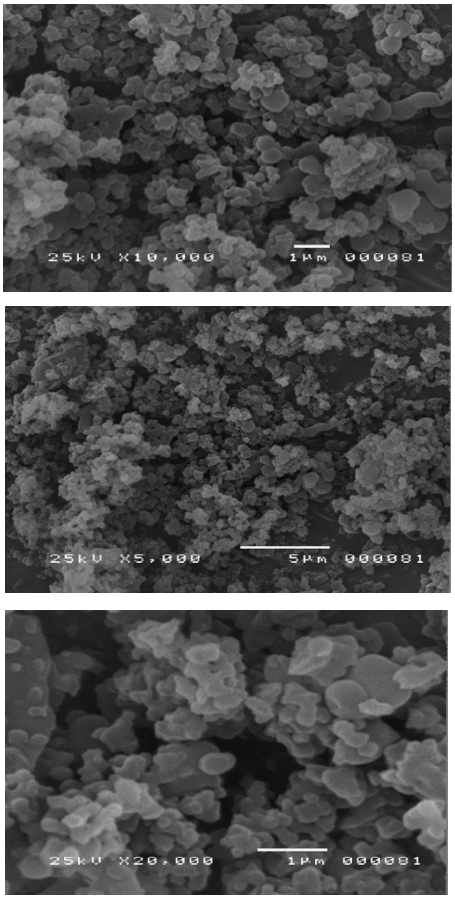

Figure 2: SEM Images of G--nZVI--Cu

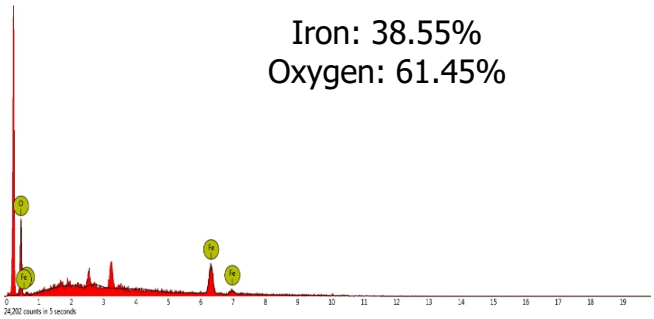

A. Trial 1

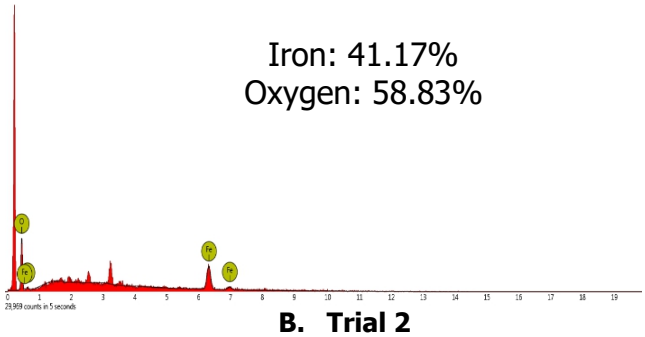

B. Trial 2

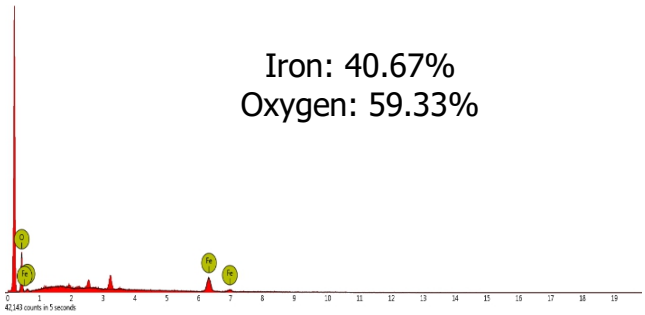

C. Trial 3

Figure 3: Energy Dispersive X--raySpectrum of G--nZVI

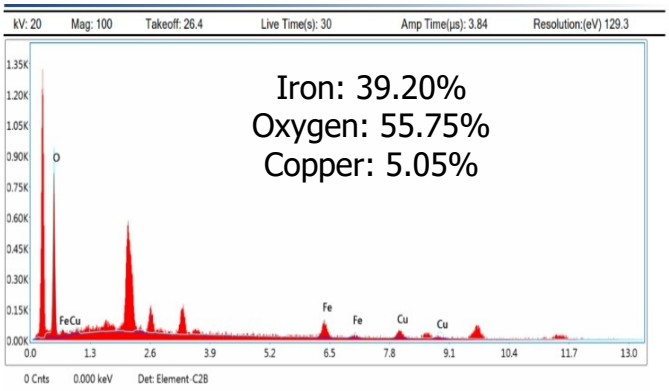

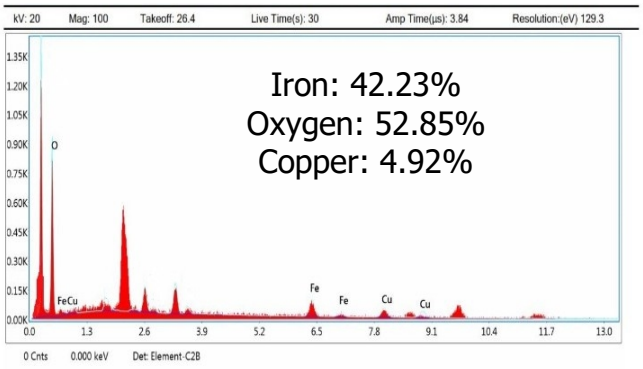

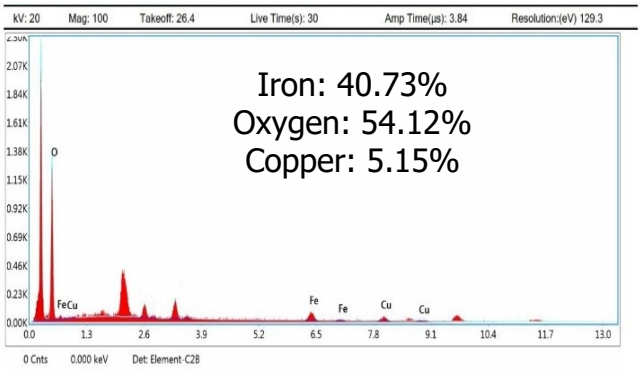

Figure 4: Energy Dispersive X--raySpectrum of G--nZVI--Cu

Figure 3 shows the elemental compositions of G--nZVI for trials 1--3. The percentage composition shows little deviations of the data from each other. The EDX spectrums has a higher peaks of oxygen. The presence of significant amount of oxygen in the analysis was due to several processes involved in the synthesis, it includes the filtration, freeze--drying, and storage of the particles. Also in Figure 5, the core shell structure of G--nZVI and G--nZVI--Cu shows that there is a thin layer of iron oxyhydroxide (FeOOH) and iron oxide (Fe_3O_4), thus adding a significant amount to the total percentage of oxygen in the particles (Vilardi and Palma, 2016).

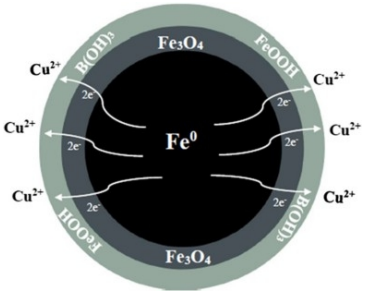

Figure 5: Core Shell Structure of G--nZVI and G--nZVI--Cu (Vilardi and Palma, 2016)

Figure 4 shows the elemental compositions of G--nZVI--Cu. There is a small percentage of copper observed by the EDX machine due to the addition of small amount of copper to the iron--copper precursor of the initial solution. The copper coating in the nZVI structure is also known to decrease the aggregation and agglomeration of G--nZVI, and enhances the reduction of nitrate in aqueous solutions (Muradova, 2016).

X--ray Diffraction Results

The crystallinity of the synthesized G--nZVI and G--nZVI--Cu was evaluated using X--ray Diffractometer. The X--ray diffraction spectra of the synthesized G--nZVI showed no clear peak corresponding to amorphous iron at around 2θ = 45°. A sharp and distinct peak indicates that the material is crystalline in structure, while the absence of sharp peak indicates that the material is amorphous, thus confirming the amorphous shape of G--nZVI and G--nZVI--Cu obtained from suganda leaves extract. Usually, iron nanoparticles synthesized by Sodium borohydride exhibits clear peaks at 2θ = 45° for zero valent iron, while on the other hand, the synthesized iron nanoparticles from suganda extract is amorphous in structure.

This result indicates that the green method of synthesizing iron nanoparticles produces amorphous structure. This property is the difference between the green nZVI and nZVI by Sodium borohydride. This difference in structure is due to the heterogeneous constituents of the extract used (Machado et al., 2015).

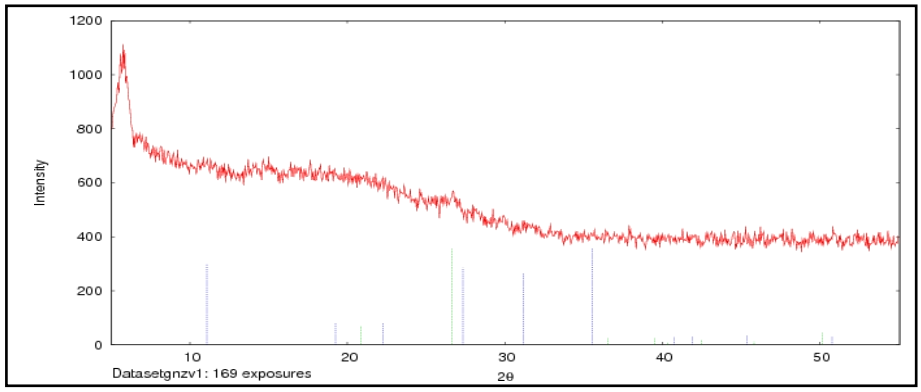

G--nZVI

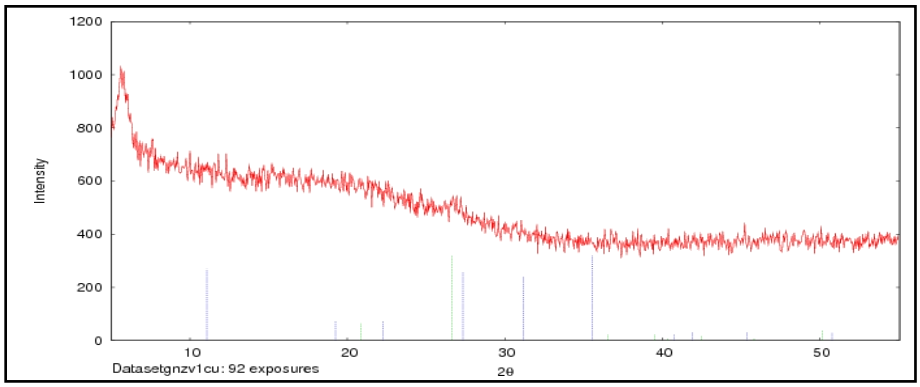

G--nZVI--Cu

Figure 6: X--ray Diffraction Spectra of Synthesized G--nZVI and G--nZVI--Cu

Nitrate Reduction Using G--nZVI And G--nZVI--Cu

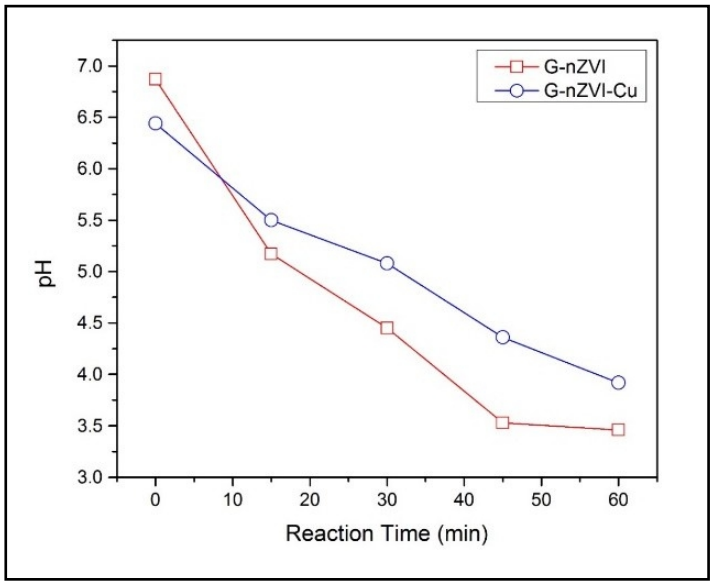

Figure 7: Reaction Time vs. pH of G--nZVI and G--nZVI--Cu

As the reaction time proceeds, a significant decrease in the solution's pH was observed. From the initial pH of G--nZVI, it drops from 6.87 to 3.46, while in the case of G--nZVI--Cu, the pH decreases from 6.44 to 3.92. It is seen from the data that the initial pH for G--nZVI was higher and has dropped significantly compared to G--nZVI--Cu. Also, small deviation of the data from each other was observed for both cases. This indicates that the reaction favors a more acidic condition of the system for both cases. Most studies also indicated that the acidic to near neutral systems were observed as the reaction time proceeds. It is known that the nitrate reduction system is a process that is surface--mediated and acid--driven (Khalil, 2015).

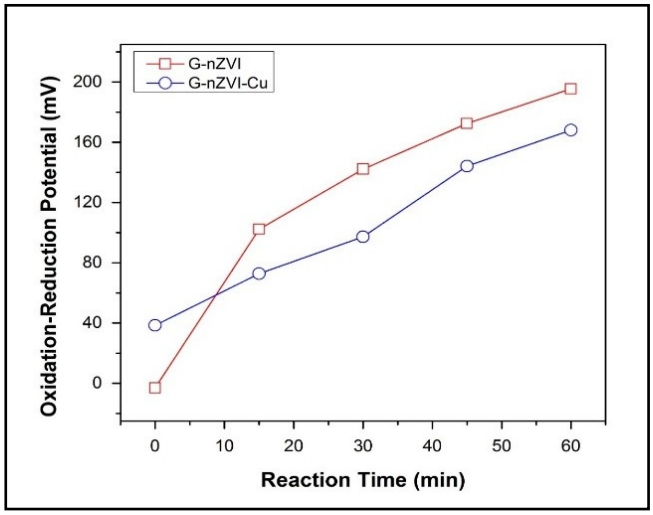

Figure 8: Graph of Reaction Time vs. Oxidation Reduction Potential for G--nZVI andG--nZVI--Cu

The oxidation--reduction potential is a way to measure a certain substance's ability to acquire or release electrons and thereby be reduced. The initial ORP of G--nZVI is --3.07 mV and 38.40 mV for G--nZVI--Cu, and rises to 195.47 mV and 168.13 mV respectively after the reaction time of 60 minutes. As the reaction time proceeds, it was observed that the ORP increases tremendously for both cases. The increase in ORP reading, suggests that the environment was oxidizing rather than reducing.

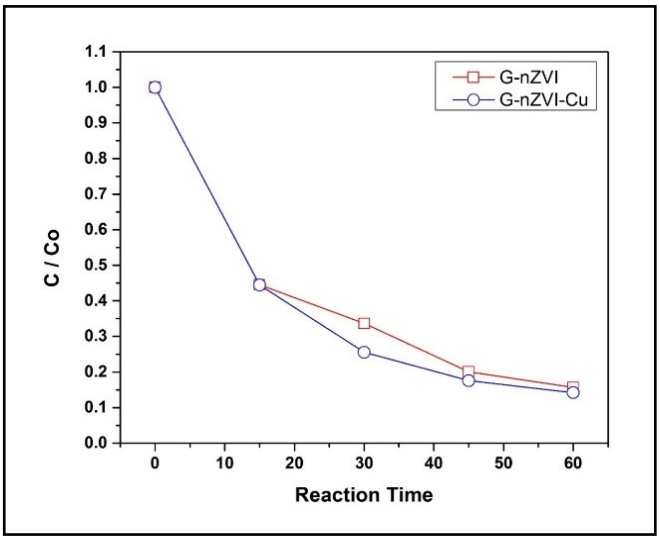

Figure 9: Graph of Reaction Time vs. C / Co for G--nZVI and G--nZVI--Cu

The graph above shows the relationship of C/Co with respect to time. C/Co was expressed in terms of residual nitrate left in the solution divided by the initial nitrate concentration in the solution. After 15 minutes, C/Co was 0.446 and 0.444 for G--nZVI and G--nZVI--Cu respectively, corresponding to more than half of the initial nitrate reduced, amounting to 267.33 and 266.67 ppm respectively. The reaction continued to proceed until the end of 60 minutes. The values of C/Co at this point was at 0.156 and 0.142 respectively, yielding to the final residual nitrate content of 93.83 ppm and 85.17 ppm for G--nZVI and G--nZVI--Cu respectively. This signifies that G--nZVI--Cu reduces more amount of nitrate content than G--nZVI, due to the addition of copper bimetal, which is a mild catalyst (Guo et al., 2017).

Using the two sample T test, one tail and two tail p--value corresponds to $p = 0.419$ and $p = 0.837$, respectively. Therefore, the data obtained for G--nZVI and G--nZVI--Cu have no significant difference with each other.

Various studies of Sodium borohydride synthesis of nZVI and nZVI--Cu show the difference of the % reduction efficiencies of the two. This can be seen in the studies of Khalil et al. in 2015, Vilardi et al. in 2016, and other various researches. However, synthesis using leaf extracts exhibited no significant difference between the reduction efficiencies. This might be due to that the copper bimetal loading was small enough to cause property change of G--nZVI particles, thus failing to fully contact nitrate during redox reaction (Guo et al., 2017).

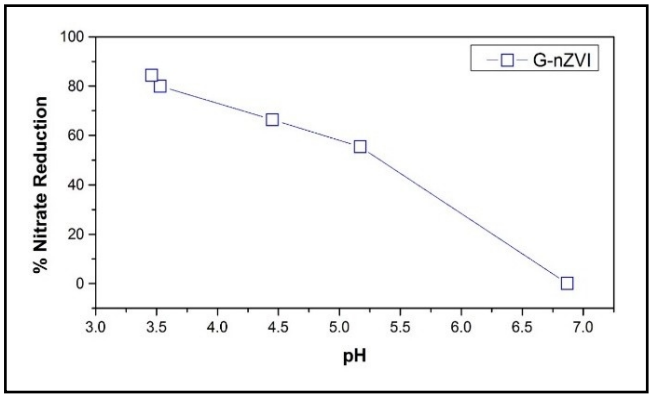

Figure 10: Graph of % Nitrate Reduction vs. pH for G--nZVI

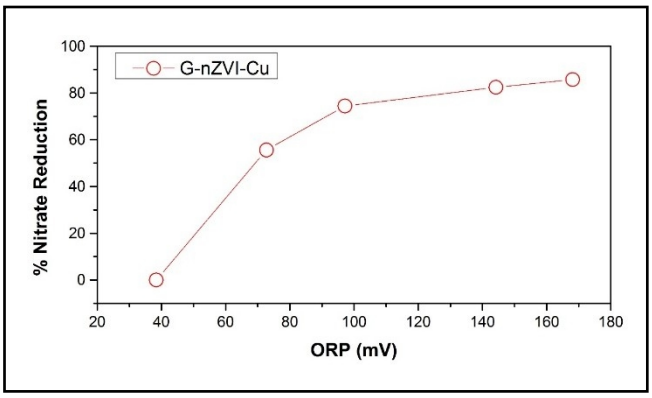

Figure 11: Graph of % Nitrate Reduction vs. ORP for G--nZVI

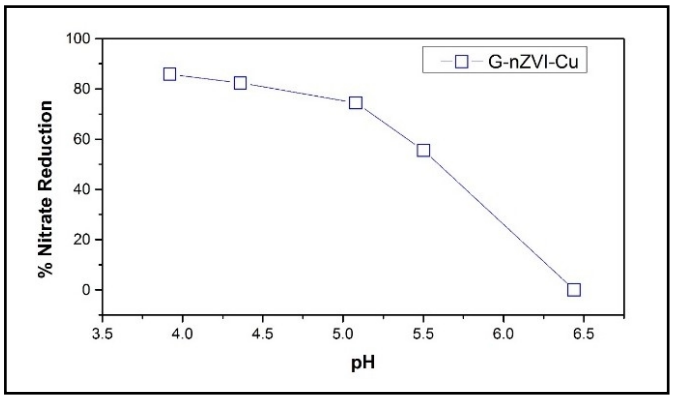

Figure 12: Graph of % Nitrate Reduction and pH for G--nZVI--Cu

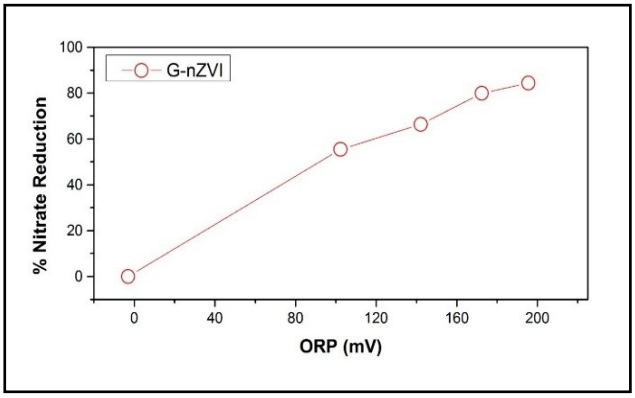

Figure 13: Graph of % Nitrate Reduction and ORP for G--nZVI--Cu

According to Figures 10, 11, 12 and 13, at the initial pH of 6.87 and 6.44 for G--nZVI and G--nZVI--Cu respectively, Oxidation--Reduction Potential (ORP) was at --3.07 and 38.40 mV. It was clearly seen that as more nitrate has been reduced, the pH fluctuates. After the reaction time of 1 hour, residual nitrate left in the solution was at 93.83 ppm and 85.17 ppm for G--nZVI and G--nZVI--Cu respectively, which amounted to 84.36% and 85.81% nitrate reduction. After 1 hour, the ORP is at 195.47 mV and 168.13 mV for G--nZVI and G--nZVI--Cu respectively. The positive ORP reading indicated that the environment has an oxidizing environment.

The data obtained suggests that the reduction of nitrate using G--nZVI and G--nZVI--Cu was more favorable in acidic conditions. At lower pH, other protective layers and Iron (II) oxide that adhered to G--nZVI and G--nZVI--Cu during the reaction would dissolve away at the G--nZVI and G--nZVI--Cu surface. This phenomenon would cause more reactive sites for the reduction of nitrate (Muradova et al., 2016).

Multiple linear regression was used to predict the % nitrate reduction using pH and ORP. In this case, the Nitrate Reduction was the dependent variable and the pH and ORP were the independent variable. The general form of the equation to predict Nitrate Reduction of G--nZVI and G--nZVI--Cu, respectively from pH and ORP was predicted as:

% Nitrate reduction = 75.712 – 10.471 (pH) – 0.243 (ORP), for G--nZVI (Eq. 1)

% Nitrate reduction = 906.682 – 129.878 (pH) – 1.826 (ORP), for G--nZVI--Cu (Eq. 2)

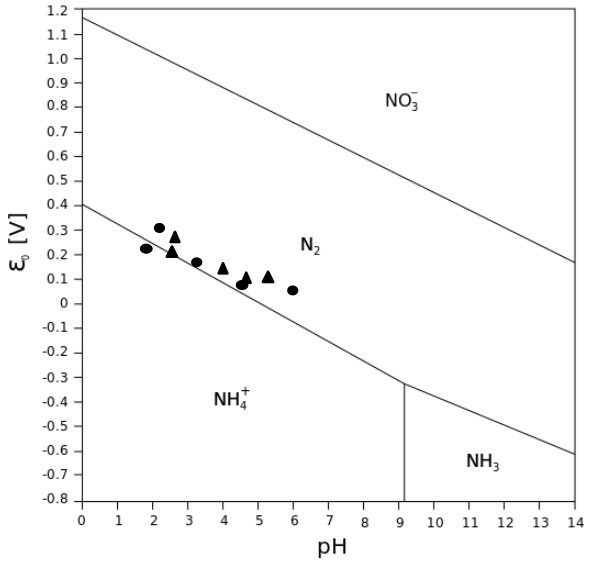

Figure 14: Pourbaix Diagram of Nitrogen (•-- G--nZVI, Δ – G--nZVI--Cu)

The relationship between pH and ORP can also be seen in the pourbaix diagram of nitrogen. It was seen that at lower pH and lower ORP, ammonium was the predominant product. Nitrogen gas was also produced in higher ORP values. The nitrogen gas formation was seen at the first 15 minutes of the reaction since it has higher pH and positive ORP. But as the reaction progresses, significant amount of

ammonium was also produced as the product of the reaction.

Ammonium and nitrogen gas were produced as the main product of the reduction of nitrate by G--nZVI and G--nZVI--Cu at pH lower than 9. Since the system was acidic, it was expected that the reaction will favor the ammonium formation rather than ammonia (Hwang et al., 2010).

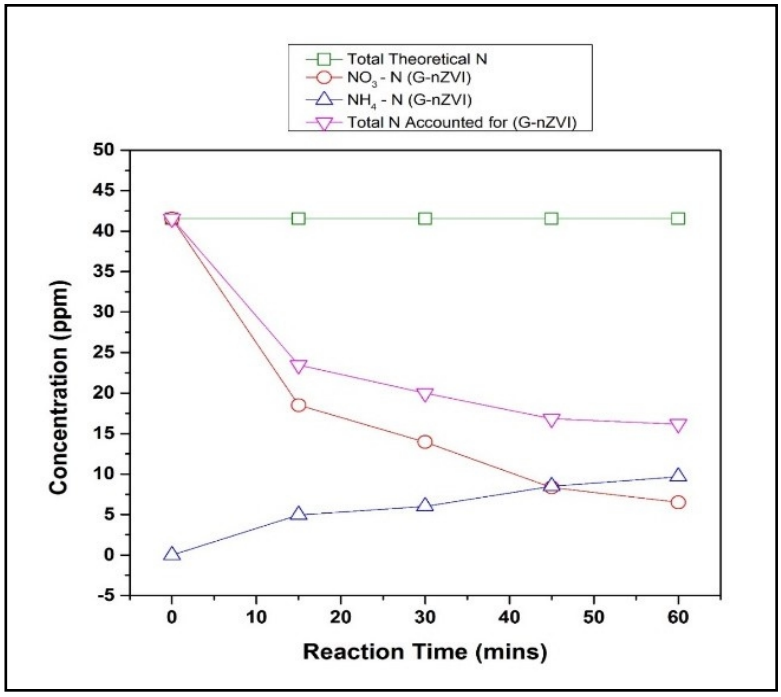

Figure 15: Nitrogen balance during the reaction of nitrate with G--nZVI

The reaction between G--nZVI and G--nZVI--Cu and nitrate can take the following reaction pathways: (Khalil et al., 2015)

$$4\,Fe^{0} + NO_{\mathrm{C}}{}^{\%} + 10\,H^{\mathrm{E}} \rightarrow 4\,Fe^{\mathrm{GE}} + NH_{\mathrm{H}}{}^{\mathrm{E}} + 3H_{\mathrm{G}}O$$
$$Fe^{0} + NO_{\mathrm{C}}{}^{\%} + 2\,H^{\mathrm{E}} \rightarrow Fe^{\mathrm{GE}} + NO_{\mathrm{G}}{}^{\%} + H_{\mathrm{G}}O$$
$$3\,Fe^{0} + NO_{\mathrm{G}}{}^{\%} + 8\,H^{\mathrm{E}} \rightarrow 3\,Fe^{\mathrm{GE}} + NH_{\mathrm{H}}{}^{\mathrm{E}} + 2\,H_{\mathrm{G}}O$$
$$3\,Fe^{0} + 2\,NO_{\mathrm{G}}{}^{\%} + 8\,H^{\mathrm{E}} \rightarrow 3\,Fe^{\mathrm{GE}} + N_{\mathrm{G(L)}} + 4H_{\mathrm{G}}$$

The possible products of the reaction between nitrate and G--nZVI and G--nZVI--Cu were ammonium, nitrogen gas and nitrite according to equations above.

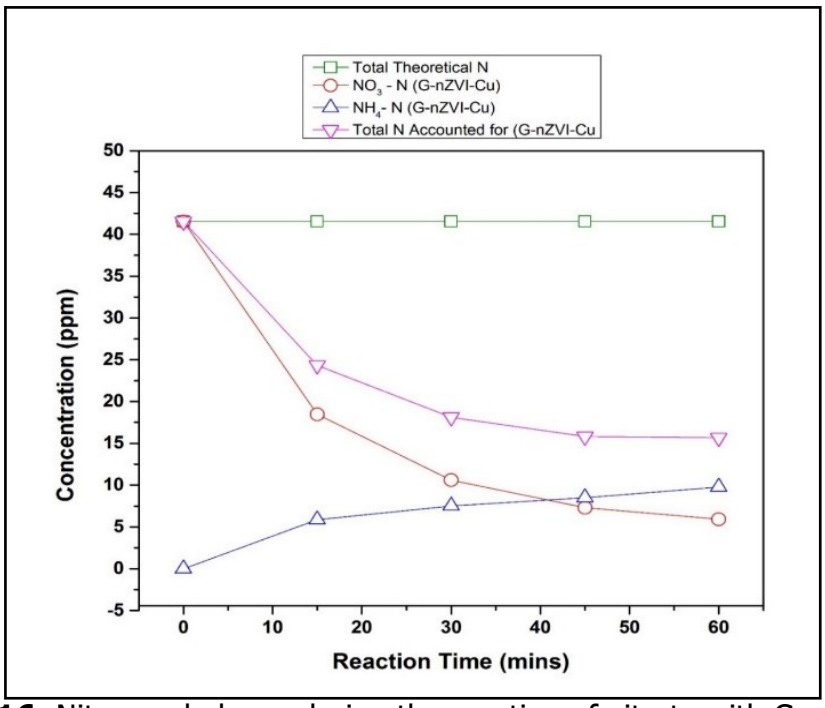

Figure 16: Nitrogen balance during the reaction of nitrate with G--nZVI--Cu

The residual nitrogen in the graph comprises of both nitrogen gas and nitrite if the reaction pathways favored these reaction products. According to the calculated nitrogen mass balance, ammonium amounted to 9.68 ppm and 9.78 ppm nitrogen for G--nZVI and G--nZVI--Cu at the end of 60 minutes. The total nitrogen accounted for was the sum of residual nitrate and ammonium during the reaction. However, the data showed that the other products of reaction, which was nitrogen gas and some nitrite produced a higher concentration than ammonium, which the two amounted as total nitrogen unaccounted for as 25.38 ppm and 25.87 ppm altogether for G--nZVI and G--nZVI--Cu. This data was supported by the pourbaix diagram of nitrogen (Figure 14), which shows that the most stable products of the reactions would be ammonium and nitrogen gas.

The reason why the N--accounted was lower than N--unaccounted is because, at very reducing conditions, ammonium was formed, while for intermediate conditions, N_2 was the stable form (Cubicciotti, 1989). The data confirms that the reaction has a higher selectivity to nitrogen gas than ammonium. This pattern was supported by the study of Lubphoo et al. in 2015.

5.0 CONCLUSIONS AND RECOMMENDATIONS

5.1 CONCLUSIONS

Effect of Temperature and Solvent Concentration on Phenolic Extraction Among the cases, case 6 (35°C, 90% ethanol) exhibited the highest absorbance indifferent extract concentrations. The ANOVA results showed that temperature andsolvent concentration has a significant effect on the phenolic extraction at all extract concentrations with a p--value < 0.05. The average total phenolic content for each cases was calculated and case 6 exhibited the highest total phenolic content, since

the temperature was much lower than the degradation temperature of the extract at 50°C.

Synthesis and Characterization of G--nZVI and G--nZVI--Cu

The SEM--EDX results showed that the particles showed chain--like formations and appear agglomerated. The particle sizes ranges from 100--150 nm, which falls under the acceptable range of nanoscale characterization. The G--nZVI particles were mainly composed of iron and oxygen, while the G--nZVI--Cu were composed of iron, oxygen and traces of copper.

The EDX machine detected higher amounts of oxygen ranging from 50--60%, iron having 40--50% weight and copper with nearly 4--5% weight. Meanwhile, the XRD results showed that G--nZVI and G--nZVI--Cu particles have no clear peak at $2\theta = 45°$, indicating that the green synthesized particles were amorphous in structure.

Nitrate Reduction using G--nZVI and G--nZVI--Cu

From the photometric analysis, significant amount of nitrate was reduced after 60 minutes, yielding to the final residual nitrate content of 93.83 ppm and 85.17 ppm for G--nZVI and G--nZVI--Cu respectively. These values corresponds to the final % nitrate reduction of 84.36% and 85.81% for G--nZVI and G--nZVI--Cu. The two sample t--test showed that $p > 0.05$, Therefore, the data obtained for G--nZVI and G--nZVI--Cu have no significant difference with each other, due to that the copper bimetal dosage is too small to cause a property change in the particles. Moreover, the pH and ORP were also monitored during the reaction time intervals. It is evident that the reaction mechanism favors acidic pH and oxidizing environment. Furthermore, the pourbaix diagram showed the stable products of the oxidation--reduction reaction. Multiple linear regression was used to predict % nitrate reduction from pH and ORP. It showed that the $R^2 = 0.982$ for G--nZVI, and $R^2 = 0.980$ for G--nZVI--Cu. These values mean that the prediction of % nitrate reduction is highly significant using pH and ORP.

The general form of the equation to predict Nitrate Reduction of G--nZVI and G--nZVI--Cu, respectively from pH and ORP was predicted as:

% Nitrate reduction = 75.712 – 10.471 (pH) – 0.243 (ORP), for G--nZVI
% Nitrate reduction = 906.682 – 129.878 (pH) – 1.826 (ORP), for G--nZVI--Cu

Since both systems has higher pH and higher ORP values, ammonium and nitrogen gas were the main products of the reaction. The nitrogen balance indicated that the nitrogen gas has a higher concentration than ammonium, which shows the higher selectivity of the reaction to nitrogen gas than ammonium.

6.0 RECOMMENDATIONS

This study can be subjected to further development. For future studies, the researchers recommend the following:

1) Use modern extraction techniques (Microwave--assisted extraction, Ultrasound--assisted extraction, etc.) for polyphenol extraction for an efficient synthesis;

2) Synthesize G--nZVI and G--nZVI--Cu particles with an extract with a higher phenolic content;
3) Varying the parameters such as copper bimetal dosage and pH to know the optimum copper bimetal loading and pH to achieve higher percentages of nitrate reduction;
4) Improve the stability of G--nZVI and G--nZVI--Cu particles during synthesis to prevent further oxidation;
5) Determine the reduction efficiency of G--nZVI and G--nZVI--Cu to actual wastewater.

7.0 REFERENCES

Determination of substances characteristic of green and black tea — Part 1: *Content of total polyphenols in tea — Colorimetric method using Folin--Ciocalteu reagent.* (2005).

Guo, X., Yang, Z., Liu, H., Lv, X., Tu, Q., Ren, Q., & Xia, X. (2015). Common oxidants activate the reactivity of zero--valent iron (ZVI) and hence remarkably enhance nitrate reduction from water. *SEPARATION AND PURIFICATION TECHNOLOGY*, 146, 227–234. https://doi.org/10.1016/j.seppur.2015.03.059

Hamid, S., Bae, S., Lee, W., Amin, M. T., & Alazba, A. A. (2015). Catalytic Nitrate Removal in Continuous Bimetallic Cu--Pd/Nanoscale Zerovalent Iron System. *Industrial and Engineering Chemistry Research,* 54(24), 6247–6257. https://doi.org/10.1021/acs.iecr.5b01127

Herlekar, M., Barve, S., & Kumar, R. (2014*). Plant--Mediated Green Synthesis of Iron Nanoparticles*, 2014.

Huang, C.--P., Wang, H.--W., & Chiu, P.--C. (2006). *Nitrate reduction by metallic iron. Water Research,* 32(8), 2257–2264. https://doi.org/10.1016/S0043--1354(97)00464--8

Hwang, Y.--H., Kim, D.--G., & Shin, H.--S. (2011). Mechanism study of nitrate reduction by nano zero valent iron*. Journal of Hazardous Materials,* 185(2--3), 1513–1521. https://doi.org/10.1016/j.jhazmat.2010.10.078

Kapoor, A., & Viraraghavan, T. (1997). *nitrate removal from drinking water--review.Pdf,* 123(APRil), 371–380.

Karimi, A., Min, B., Brownmiller, C., & Lee, S.--O. (2014). Effects of Extraction Techniques on Total Phenolic Content and Antioxidant Capacities of Two Oregano Leaves. *Journal of Food Research.* https://doi.org/10.5539/jfr.v4n1p112

Khalil, A. M. E., Eljamal, O., Jribi, S., & Matsunaga, N. (2016). Promoting nitrate reduction kinetics by nanoscale zero valent iron in water via copper salt addition. *Chemical Engineering Journal*, 287, 367–380. https://doi.org/10.1016/j.cej.2015.11.038

Krasae, N., Wantala, K., Tantriratna, P., & Grisdanurak, N. (2014). Removal of Nitrate by Bimetallic Copper--Nanoscale Zero--Valent Iron (Cu--nZVI): Using 2 k Full Factorial Design, 36(2), 15–23.

Liou, Y. H., Lo, S., Lin, C., Kuan, W. H., & Chi, S. (2005). Chemical reduction of an unbuffered nitrate solution using catalyzed and uncatalyzed nanoscale iron particles, 127, 102–110. https://doi.org/10.1016/j.jhazmat.2005.06.029

Liu, A., Liu, J., & Zhang, W. (2015). Chemosphere Transformation and composition evolution of nanoscale zero valent iron (nZVI) synthesized by borohydride reduction in static water. CHEMOSPHERE, 119, 1068–1074. https://doi.org/10.1016/j.chemosphere.2014.09.026

M. JP, E. quality standards for water pollution. (2015). environmental WQS.pdf.

Machado, S., Pacheco, J. G., Nouws, H. P. A., Albergaria, J. T., & Delerue--Matos, C. (2015). Characterization of green zero--valent iron nanoparticles produced with tree leaf extracts. Science of the Total Environment, 533, 76–81. https://doi.org/10.1016/j.scitotenv.2015.06.091

Mohammadlou, M., Maghsoudi, H., & Jafarizadeh--Malmiri, H. (2016). A review on green silver nanoparticles based on plants: Synthesis, potential applications and eco--friendly approach. International Food Research Journal, 23(2), 446–463.

Muradova, G. G., Gadjieva, S. R., Di, L., & Vilardi, G. (2016). Nitrates Removal by Bimetallic Nanoparticles in Water, 47, 205–210. https://doi.org/10.3303/CET1647035

Nadagouda, M. N., Castle, A. B., Murdock, R. C., Hussain, S. M., & Varma, R. S. (2010). In vitro biocompatibility of nanoscale zerovalent iron particles (NZVI) synthesized using tea polyphenols. Greem Chemistry, 12(Copyright (C) 2014 American Chemical Society (ACS). All Rights Reserved.), 114–122. https://doi.org/10.1039/b921203p

Namasivayam, S., & Raju, S. (2013). Synthesis, Characterization and Anti Bacterial Activity of Chitosan Stabilized Nano Zero Valant Iron. Bulletin of Pharmaceutical and …, 1(1), 7–11.

Njagi, E. C., Huang, H., Stafford, L., Genuino, H., Galindo, H. M., Collins, J. B., … Suib, S. L. (2011). Biosynthesis of Iron and Silver Nanoparticles at Room Temperature Using Aqueous Sorghum Bran Extracts, 27(17), 264–271. https://doi.org/10.1021/la103190n

Oregano Shown to be the Most Powerful Culinary Herb -- NaturalNews.com. (n.d.).
Oxidation--Reduction Reactions: Redox. (n.d.).

Pattanayak, M., & Nayak, P. L. (2012). Ecofriendly Green Synthesis Of Iron Nanoparticles From Various Plants And Spices Extract. P . L . Nayak Research Foundation and Centre for Excellence in Nano Science and Technology , Synergy Institute of Technology, 68–78.

Proestos, C., Lytoudi, K., Mavromelanidou, O., Zoumpoulakis, P., & Sinanoglou, V. (2013). Antioxidant Capacity of Selected Plant Extracts and Their Essential Oils. Antioxidants, 2(1), 11–22. https://doi.org/10.3390/antiox2010011

Sparis, D., Mystrioti, C., Xenidis, A., & Papassiopi, N. (2015). Desalination and Water Treatment Reduction of nitrate by copper--coated ZVI nanoparticles, (January), 37–41. https://doi.org/10.1080/19443994.2012.748303

Sparr Eskilsson, C., & Björklund, E. (2000). Analytical--scale microwave--assisted extraction. Journal of Chromatography A, 902(1), 227–250. https://doi.org/10.1016/S0021--9673(00)00921--3

Sravanthi, M., Ku, D. M., Ravichandra, M., Vasu, G., & Hemalatha, K. P. J. (2016). International Journal of Current Research and Academic Review, 4(8), 30–44.

Sun, Y.--P., Li, X., Cao, J., Zhang, W., & Wang, H. P. (2006). Characterization of zero--valent iron nanoparticles. Advances in Colloid and Interface Science, 120, 47–56. https://doi.org/10.1016/j.cis.2006.03.001

Wang, X., Le, L., Alvarez, P. J. J., Li, F., & Liu, K. (2015a). Journal of the Taiwan Institute of Chemical Engineers Synthesis and characterization of green agents coated Pd / Fe bimetallic nanoparticles. Journal of the Taiwan Institute of Chemical Engineers, 50, 297–305. https://doi.org/10.1016/j.jtice.2014.12.030

Wang, X., Le, L., Alvarez, P. J. J., Li, F., & Liu, K. (2015b). Synthesis and characterization of green agents coated Pd/Fe bimetallic nanoparticles. Journal of the Taiwan Institute of Chemical Engineers, 50, 297–305. https://doi.org/10.1016/j.jtice.2014.12.030

Wissam, Z., Ghada, B., Wassim, A., & Warid, K. (2012). Effective extraction of polyphenols and proanthocyanidins from Pomegranate's peel. International Journal of Pharmacy and Pharmaceutical Sciences, 4(SUPPL.3), 675–682.

World Health Organization. (2007). Nitrate and Nitrite in Drinking Water. Background Document for Development of WHO Guidelines for Drinking Water Quality, 31. https://doi.org/10.1159/000225441

Yuris, A., & Siow, L.--F. (2014). A Comparative Study of the Antioxidant Properties of Three Pineapple (Ananas comosus L.) Varieties. Journal of Food Studies, 3(1), 40. https://doi.org/10.5296/jfs.v3i1.4995

Yuvakkumar, R., Elango, V., Rajendran, V., & Kannan, N. (2011). Preparation and characterization of zero valent Iron nanoparticles*. Digest Journal of Nanomaterials* and Biostructures, 6(4), 1771–1776.

Zhang, J., Hao, Z., Zhang, Z., Yang, Y., & Xu, X. (2010). Kinetics of nitrate reductive denitrification by nanoscale zero--valent iron. *Process Safety and Environmental Protection*, 88(6), 439–445. https://doi.org/10.1016/j.psep.2010.06.002

Zhu, I., & Getting, T. (2016). *A review of nitrate reduction using inorganic materials,* 2515(August). https://doi.org/10.1080/09593330.2012.706646

Ziajahromi, S., Zand, A. D., & Khanizadeh, M. (2012*). Nitrate Removal from Water Using Synthesis Nanoscale Zero--Valent Iron* (NZVI), 105–110.

Zin, M. T., Borja, J., Hinode, H., & Kurniawan, W. (2013). *Synthesis of Bimetallic Fe / Cu Nanoparticles with Different Copper Loading Ratios,* 7(12), 1031–1035.